COMPARISON OF DESIGN FEATURES OF QUADROTOR AIRCRAFT AND HELICOPTERS FROM THE POINT OF VIEW OF FLIGHT PERFORMANCE

Dong Han, donghan@nuaa.edu.cn, College of Aerospace Engineering, Nanjing University of Aeronautics and Astronautics, Nanjing 210016, China

George N. Barakos, George.Barakos@glasgow.ac.uk, CFD Laboratory, School of Engineering, University of Glasgow, G12 8QQ, Scotland, UK

Abstract

Blade flapping, control methods and rotor/rotor aerodynamic interference are some of the main differences between quadrotor aircraft and helicopters. To investigate these differences in flight performance of square formation quadrotor aircraft, a performance prediction model, including a validated rotor model, an aerodynamic model, and a propulsive trim model, is used. The square formation quadrotor aircraft with variable blade pitch or rotor speed as control means are analyzed. Compared with a helicopter rotor, from low to medium speed flight, the aerodynamic interference between the front and rear rotors dominates the power difference between quadrotors and helicopters. At high speed flight, the blade flapping and aerodynamic interference can lead to increased power, and the blade flapping can be more pronounced. Applying cyclic pitch controls in quadrotor aircraft can effectively control the blade flapping, reduce the rotor power, and increase the maximum forward speed. In general, the overall rotor power consumption of quadrotor aircraft is larger than the equivalent helicopter rotor.

NOMENCLATURE

C_{M_y}	pitching moment coefficient, dimensionless
D	fuselage drag, N
F	force, N
H	rotor drag force, N
k	cross-induced velocity factor, dimensionless
L_x	longitudinal distance from the rotor shaft to the mass center of the aircraft, m
L_y	lateral distance from the rotor shaft to the mass center of the aircraft, m
L_z	vertical distance from the rotor plane to the mass center of the aircraft, m
M_x	rolling moment, Nm
M_y	pitching moment, Nm
P	rotor power, W
q	dynamic pressure, Pa
Q	rotor torque, Nm
R	rotor radius, m
T	rotor thrust, N
t	time, s
V_∞	magnitude of free stream velocity, m/s
v_i	induced velocity, m/s
w	damping factor, dimensionless
W	weight, N
Y	rotor side force, N
α_F	longitudinal tilt of fuselage, rad
β	blade flapping angle, rad
θ_0	collective pitch, rad
θ_{1c}	lateral cyclic pitch, rad
θ_{1s}	longitudinal cyclic pitch, rad
κ	self-induced velocity factor
ρ	air density, kg/m^3
ψ	azimuth angle, rad
Ω	rotor speed, rad/s

subscripts

F	contribution from fuselage
1-4	rotor index

superscripts

$\dot{()}$	$d()/dt$

1. INTRODUCTION

Quadrotor aircraft weighting several kilograms have been widely applied in aerial photography, recreation, observation and other areas. Due to their excellent controllability, quadrotor aircraft are now expanding their application in transportation, search and rescue, communication and so on. Their size becomes larger, and their weight becomes heavier. However, certain limitations in flight performance, such as payload, endurance, range and so on, make their adoption difficult. An effective way to solve this problem is to reduce the power consumption of quadrotor aircraft, and improve the flight performance. Understanding the design features of quadrotor aircraft and their potential effects on the flight performance is paramount for

the selection of effective means to reduce the rotor power. The efficiency of quadrotor aircraft compared with helicopters is another interesting question, since they all belong to vertical takeoff and landing aircraft.

Almost all past research on quadrotor aircraft focused on flight dynamics and control. Most of the times, simple estimates of rotor thrust and rotor torque are used [1-6]. The rotor thrust and torque are assumed to be proportional to the square of the rotor speed. These models can not consider the effects of air compressibility and stall on the rotor aerodynamics, and blade flapping is usually not taken into account, which is paramount for the aerodynamics of flexible rotors in edgewise flight. It is obvious that these models need improvemets for the prediction and analysis of the flight performance of quadrotor aircraft.

Luo et al. proposed a novel forward flight model for quadrotor aircraft with a wake interference model [7], that could provide consistent trends with CFD analyses. Hwang et al. investigated the aerodynamic interactions among the rotors of quadrotor aircraft using CFD [8]. The results showed that the aerodynamic interactions among the rotors needed to be considered in the design of the flight control system. Misiorowski et al. confirmed the strong interference between the front and rear rotors of quadrotor aircraft [9]. Their study showed that the rear rotor performance was lowered by the wake trailed from the front rotor of the quadrotor [10]. It is obvious that the aerodynamic interference due to the multi-rotor configuration is a key feature of quadrotor aircraft. Quadrotors change the thrusts of each of their rotors for control by adjusting rotor speed or blade pitch. Niemiec and his coworkers developed a flight dynamics model of a 2kg quadrotor helicopter based on the blade element theory [11, 12]. Variable speed rotor consumed less power than variable blade pitch, so the control method may have significant influence on the flight performance, which is a different from helicopters.

Quadrotor aircraft remove cyclic pitch controls from their rotor systems, to simplify the system and reduce weight. Without cyclic pitch controls, the blade flapping is uncontrolled. At hover or low speed flight, the longitudinal and lateral blade flapping may be not an issue. If, however, large longitudinal or lateral flapping occurs at a rotor system, this may lower the flight performance. In past research efforts, the blades of quadrotor aircraft are usually treated as rigid bodies, since the blades are very stiff for small scale quadrotor aircraft. The blade flapping is usually not considered in the modeling. However, large rotor blades could not be designed to be very stiff. If the quadrotor blades are made similar to helicopter rotor blades, the blade flapping motion has to be considered in edgewise flight. Removing the cyclic pitch controls from the rotor systems is an important design difference from helicopter rotors.

This work considered the whole aircraft trim, blade flapping and aerodynamic interference between the front and rear rotors. The effects of air compressibility and stall on the rotor aerodynamics are considered in the rotor model. The design features of quadrotor aircraft, which are different from helicopters from the point of view of flight performance, are also explored. Blade flapping, aerodynamic interference and trim method are investigated by comparing the performance with helicopter rotors. Cyclic pitch controls are also used to reduce the power consumption and improve the flight performance.

2. FLIGHT PERFORMANCE MODEL

2.1. Rotor Model

The blade model is based on a rigid beam with a hinge offset and a hinge spring, which is used to match the fundamental flapwise blade frequency. Look-up table aerofoil aerodynamics is used to calculate the lift and drag coefficients of blade elements according to the local resultant air flow and angle of attack, which can capture air compressibility and stall effects. The local resultant air flow consists of the forward speed of the aircraft, the motion of the blade, and the induced velocity. The induced velocity over the rotor disk is predicted by the Pitt–Peters inflow model [13], which captures the first harmonic variation of induced velocity in azimuth. The rotor model is described in Ref. 14.

The rotor model is rotating in the counter-clockwise direction. For the rotors rotating in the clockwise direction, the same rotor models are used, but the directions of the side force, rolling moment and rotor torque need to be modified to the opposite direction. In the following analysis, the distribution of the angle of attack of blade segments is presented in the counter-clockwise direction for the convenience of comparison.

2.2. Propulsive Trim

For the square formation quadrotor aircraft, usually, the fuselages are symmetry about the centerline of the vehicle, so the side force and the rolling moment acting on the fuselage can be assumed to be zero. Even if the lift generated by the fuselage is omitted, the drag, weight and pitching moment on the fuselage must be considered, as shown in Figure 1. The four rotors are named as ROTOR 1, ROTOR 2, ROTOR 3, and ROTOR 4 according to their locations, as shown in Figure 1. The rotor hub forces and moments and their corresponding directions are also shown in the figure. Due to the different rotation direction, the

side forces, rolling moments and torques on ROTOR 1 and ROTOR 4 are different from those acting on ROTOR 2 and ROTOR 3.

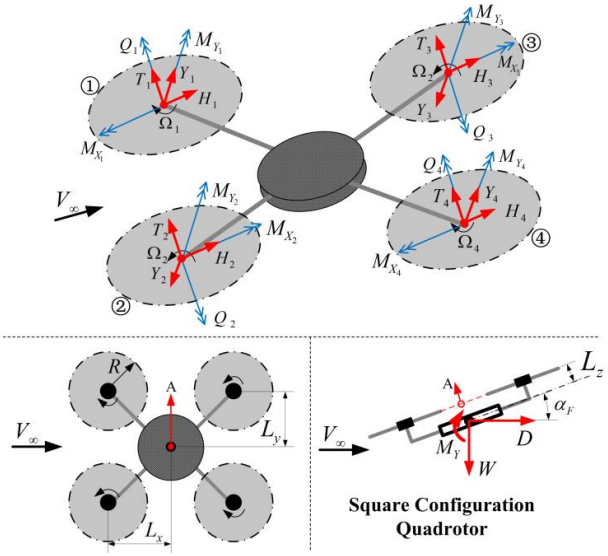

Figure 1 Forces and moment on the fuselage.

Due to the symmetry of the quadrotor aircraft, the six equilibrium equations for the quadrotor can be reduced to the following three equations:

(1) $$2(T_1+T_3)\cos\alpha_F + 2(H_1+H_3)\sin\alpha_F = W,$$

(2) $$2(T_1+T_3)\sin\alpha_F - 2(H_1+H_3)\cos\alpha_F = D,$$

(3) $$2(T_3-T_1) = \frac{2(M_{y_1}+M_{y_3})}{L_x} + \frac{(W\sin\alpha_F - D\cos\alpha_F)L_z + M_{y_F}}{L_x}.$$

If the quadrotor aircraft uses blade pitch for control, the previous three equilibrium equations can be used to obtain the collective pitch angles of ROTORs 1 and 3, i.e. $\theta_0^{(1)}$ and $\theta_0^{(3)}$, and the longitudinal tilt of the fuselage α_F. Combining Equations (5) and (6), the longitudinal tilt of the fuselage can be expressed as:

(4) $$\alpha_F = \tan^{-1}\left(\frac{\frac{D}{2}+(H_1+H_3)\cos\alpha_F}{\frac{W}{2}-(H_1+H_3)\sin\alpha_F}\right).$$

The following iterative algorithm is proposed to obtain the converged value of the longitudinal tilt of the fuselage, using

(5) $$(\alpha_F)_{n+1} = \tan^{-1}\left(\frac{\frac{D}{2}+[(H_1)_n+(H_3)_n]\cos(\alpha_F)_n}{\frac{W}{2}-[(H_1)_n+(H_3)_n]\sin(\alpha_F)_n}\right).$$

Combining Equations (5) and (7), the rotor thrusts T_1 and T_3 can be obtained by

(6) $$T_1 = \frac{W}{4\cos\alpha_F} - \frac{(H_1+H_3)\sin\alpha_F}{2\cos\alpha_F} - \frac{(M_{y_1}+M_{y_3})}{2L_x} - \frac{(W\sin\alpha_F - D\cos\alpha_F)L_z + M_{y_F}}{4L_x} = T_A,$$

and

(7) $$T_3 = \frac{W}{4\cos\alpha_F} - \frac{(H_1+H_3)\sin\alpha_F}{2\cos\alpha_F} + \frac{(M_{y_1}+M_{y_3})}{2L_x} + \frac{(W\sin\alpha_F - D\cos\alpha_F)L_z + M_{y_F}}{4L_x} = T_B.$$

To obtain the converged values of the collective pitch angles, the Newton's method is used to solve Equations (10) and (11), and the iterative expressions are

(8) $$\left(\theta_0^{(1)}\right)_{n+1} = \left(\theta_0^{(1)}\right)_n - w\,[(T_1)_n - (T_A)_n]/\left(\frac{\partial T_1}{\partial\theta_0^{(1)}}\right)_n,$$

and

(9) $$\left(\theta_0^{(3)}\right)_{n+1} = \left(\theta_0^{(3)}\right)_n - w\,[(T_3)_n - (T_B)_n]/\left(\frac{\partial T_3}{\partial\theta_0^{(3)}}\right)_n,$$

where, w is an empirical damping factor to enhance the convergence of the iteration and reduce the computation time. A value of 0.5 is used in this work.

If the quadrotor aircraft uses rotor speeds for control, the rotor speeds can be obtained by

(10) $$(\Omega_1)_{n+1} = (\Omega_1)_n - w\,[(T_1)_n - (T_A)_n]/\left(\frac{\partial T_1}{\partial\Omega_1}\right)_n,$$

and

(11) $$(\Omega_3)_{n+1} = (\Omega_3)_n - w\,[(T_3)_n - (T_B)_n]/\left(\frac{\partial T_3}{\partial\Omega_3}\right)_n.$$

2.3. Aerodynamic Interference Model

A theoretical formula on the basis of the Biot-Savart law is used to predict the aerodynamic interferences between the rotors, which is validated by the experimental results [10]. This method has been extended to consider the aerodynamic interferences for multi-rotors in forward flight [15]. At a forward speed (rotor advanced ratio $\mu > 0.1$), a lifting rotor can be modeled as a circular fixed wing [16, 17]. A horseshoe vortex is trailed from the retreating and advancing sides. This aerodynamic interference model is based on the Biot-Savart law, and assumes that the horseshoe vortex trailed from one rotor induces additional downwash to the other rotor. For a quadrotor aircraft, the induced velocity over the rotors can be expressed as

(12) $$\begin{Bmatrix} v_i^{(1)} \\ v_i^{(2)} \\ v_i^{(3)} \\ v_i^{(4)} \end{Bmatrix} = \begin{bmatrix} \kappa_1 & k_{12} & k_{13} & k_{14} \\ k_{21} & \kappa_2 & k_{23} & k_{24} \\ k_{31} & k_{32} & \kappa_3 & k_{34} \\ k_{41} & k_{42} & k_{43} & \kappa_4 \end{bmatrix} \begin{Bmatrix} v_{i0}^{(1)} \\ v_{i0}^{(2)} \\ v_{i0}^{(3)} \\ v_{i0}^{(4)} \end{Bmatrix},$$

where, the superscript 1 to 4 denotes the index of the rotors, and the subscript '0' denotes the velocity of an isolated rotor. k_{ij} denotes the cross-induced velocity factor generated by the *j*th rotor to the *i*th rotor.

2.4. Model Validation

The flight data of the UH-60A helicopter [18] is utilized to validate the rotor model used in this work. The parameters of the main rotor are listed in Table 1 [19, 20]. The fuselage drag equation utilized in the analysis is [18]

(13) $$\frac{D}{q}\,(\mathrm{ft}^2) = 35.83 + 0.016 \times (1.66\alpha_F)^2.$$

The distance between the hub center of the tail rotor and the main rotor shaft is 9.9263m. The vertical distance from the mass center of the helicopter to the rotor hub is 1.77546m. The comparison between the predictions of the rotor power with the flight test data for the takeoff weight coefficient of 0.0074 is shown in Figure 2, and the predictions by the present method are generally in good agreement with the flight test data for the cases considered.

Table 1: Main rotor parameters [19, 20]

Main Rotor Radius	8.1778 m
Main Rotor Speed	27.0 rad/s
Blade Chord Length	0.5273 m
Blade Twist	Nonlinear
Blade Airfoil	SC1095/SC1094R8
Number of Blades	4
Flap Hinge Offset	0.381 m
Blade Mass per Unit Length	13.92 kg/m
Longitudinal Shaft Tilt	3°

Since this work focuses on fundamentals, the rotors of the baseline quadrotor aircraft are the same as the UH-60A rotor without cyclic pitch controls for convenience. The takeoff weight is assumed to be 4 times the UH-60A helicopter and a weight of 37899kg is used as the baseline. The fuselage drag is also 4 times the fuselage drag of UH-60A helicopter shown in Equation 13. The pitching moment coefficient of the fuselage is defined as

(14) $$C_{M_{y_F}} = \frac{M_{y_F}}{\frac{1}{2}\rho V_\infty^2 (\pi R^2)(2L_x)}.$$

A moment coefficient of -0.03 is used, and for the quadrotor aircraft investigated, L_x and L_y are both set to be $2.0R$.

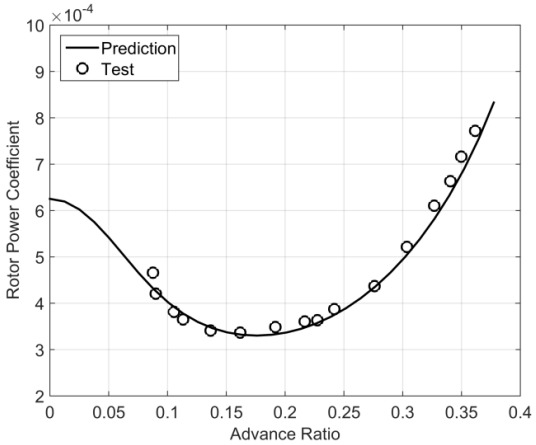

Figure 2 Comparison of predictions with flight test data.

3. VARIABLE BLADE PITCH

In this section, control means varying the blade pitch. Figure 3 shows the rotor power and corresponding power increase with forward speed. The power changes of the front and rear rotors are relative to the corresponding helicopter rotor. The figure suggests the following conclusions:

1) At low speed flight without aerodynamic interference, the front and rear rotors have almost identical power consumption as the helicopter rotor. With interference, the front rotor power decreases by 2.55%, and the rear rotor power increases by 11.2% at a speed of 50km/h. The aerodynamic interference is beneficial to the front rotor and harmful to the rear rotor. The total power of the quadrotor aircraft is larger than 4.0 times the helicopter rotor, which indicates that aerodynamic interference is not beneficial.

2) With increasing the forward speed, the rotor power of the quadrotor aircraft first decreases, and then increases. At medium speeds, a minimum value appears, which corresponds to the economic speed. The aerodynamic interference has strong influence on the front and rear rotors, especially on the rear rotor at medium speeds, which is due to the different relative locations of the rotor powers. The increment of the rear rotor power increases with the forward speed, and then decreases. At medium speeds, it can reach the maximum value, since the wake trailed from the front rotor approaches closer

to the rear rotor. Without the aerodynamic interference, the front or rear rotor power has relatively small change compared with the helicopter rotor power at low to medium speed flight.

3) At high speeds, the front and rear rotor powers are much larger than the helicopter rotor. At a speed of 250km/h, the front rotor power increases by 25.1% (381.0kW), and the value for the rear rotor is 10.7% (162.4kW) without the aerodynamic interference. With the interference, the increments for the front and rear rotors are 25.6% (388.5kW) and 19.5% (297.0kW). It is obvious that some other factor (not only the aerodynamic interference) also causes the power increase at high speed flight.

4) In general, the aerodynamic interference has significant influence on the rotor performance, especially on the rear rotor, which is due to the design feature of multi-rotor configuration. Two key parameters can influence the aerodynamic interference. One is the flight state, and the other is the distance between the rotors. Selecting a suitable flight speed can avoid strong aerodynamic interference. Increasing the distance between the front and rear rotors weakens the aerodynamic interaction, but a weight penalty may be paid.

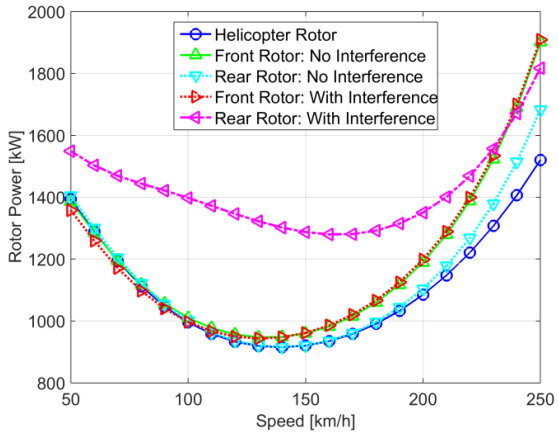

(a) rotor power

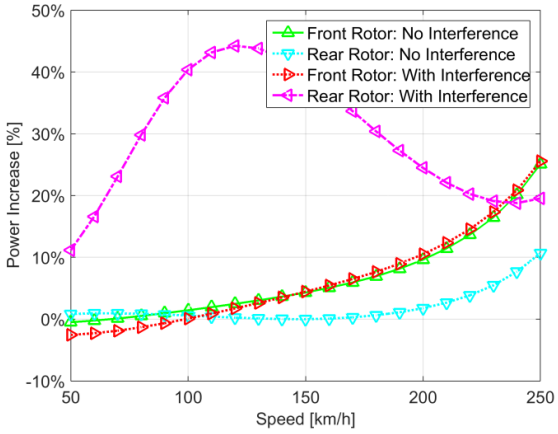

(b) power increase

Figure 3 Rotor power and corresponding power increase with forward speed.

At high speed flight, the parasitic power is the major contributor to the total power. Equation 13 indicates that the longitudinal tilt may lead to power differences at high speed flight. Figure 4 shows the longitudinal tilt of the fuselage with the forward speed. It is clear that the quadrotor aircraft has much larger longitudinal tilt than the helicopter, which indicates that the quadrotor aircraft will consume more parasitic power than the helicopter. The aerodynamic interference has little influence on the longitudinal tilt of the quadrotor aircraft, since it primarily causes the change in the rotor induced power.

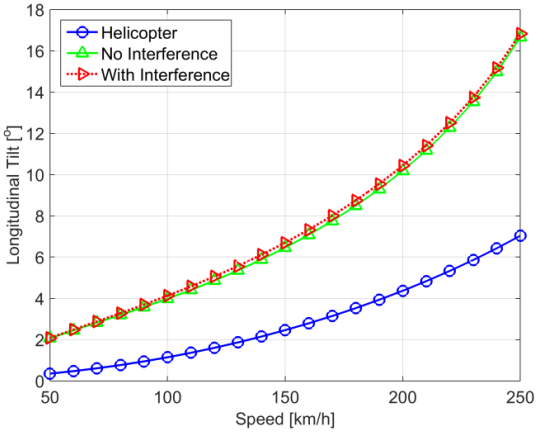

Figure 4 Longitudinal tilt with forward speed.

Since the fuselage drag of the quadrotor aircraft is balanced by all rotors, every rotor provides different propulsive force. The parasitic power balanced by a rotor is defined as

$$P_{Pi} = (T_i \sin \alpha_F - H_i \cos \alpha_F) V_\infty \quad (15)$$

Figure 5 shows the parasitic power with the forward speed. It is clear that the rotors of the quadrotor aircraft usually consume more parasitic power than helicopter rotors. The front rotor power is larger than the rear rotor. Without the interference, the parasitic powers of the front and rear rotors increase by 236.7kW and 166.4kW at a speed of 250km/h. The increase in the parasitic power is not the total increase in the front rotor power. With interference, the values are 255.6kW and 155.9kW. The larger longitudinal tilt leads to an increase in parasitic power, but it is not the only contributor to the power increase observed. The rotor profile and/or induced power increase simultaneously.

Equation 2 indicates that the increase in the fuselage or rotor drag can lead to an increase in the longitudinal tilt of the fuselage, which in turn may lead to an increase in fuselage drag. Figure 6 shows the rotor drag with forward speed. The rotor drag contributions of the quadrotor aircraft are

unusually much larger than helicopter rotors, which suggested that the quadrotor aircraft rotors are operating in a more severe aerodynamic environment. At high speed flight, the drag of the front rotor becomes larger than the rear rotor. The aerodynamic inference has relatively small influence on the rotor drag.

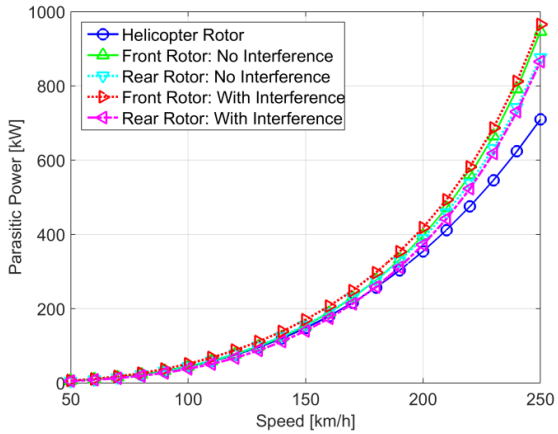

Figure 5 Parasitic power with forward speed.

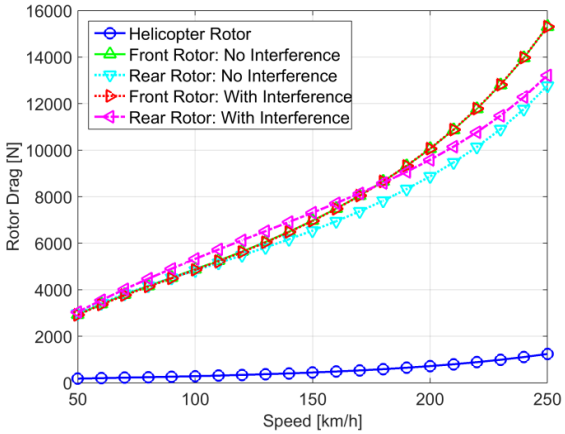

Figure 6 Rotor drag with forward speed.

Figure 7 shows the distribution of the angle of attack over the rotor disk at a speed of 250km/h with the aerodynamic interference. An intuitive impression is that the rotors of the quadrotor aircraft see larger angle of attack in the retreating side, especially for the front rotor. The rotors of the quadrotor aircraft operate in a more severe aerodynamic environment than the helicopter rotor. It can lead to the increase in the rotor drag and rotor power, and the performance naturally degrades. In the front part of the rotor disk of the quadrotor aircraft, the angle of attack is larger than the helicopter rotor, which indicates the corresponding lift at the front part can be larger. The higher lift at the front part may lead to a larger nose up pitching moment, and affect the aircraft trim.

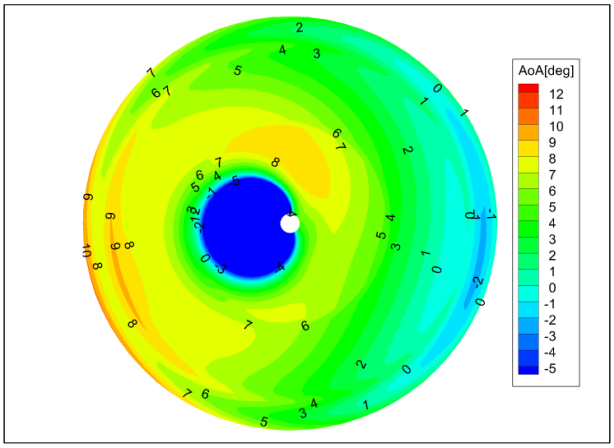

(a) helicopter rotor

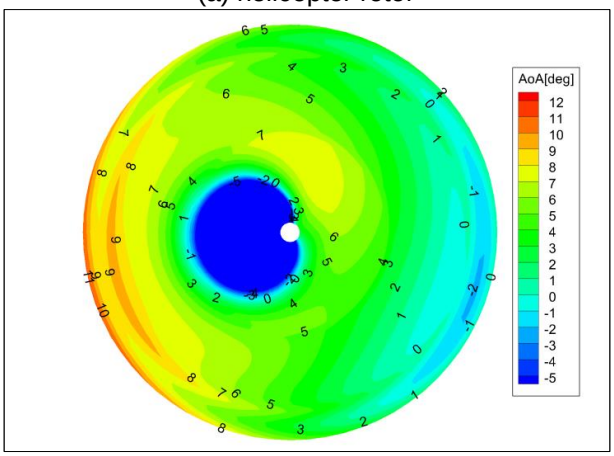

(b) front quadrotor

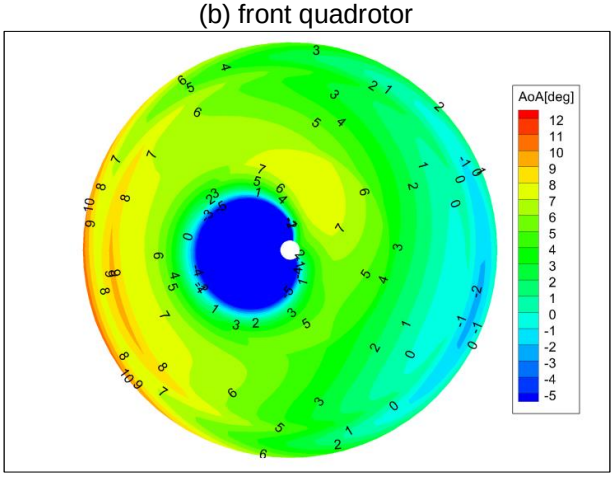

(c) rear quadrotor

Figure 7 The distribution of the angle of attack over the rotor disk.

Figure 8 shows the rotor induced and profile powers with forward speed. Without the aerodynamic interference, the change of the induced power is relatively small from low to medium speed flight, and becomes pronounced at high speed flight. With aerodynamic interference, the induced power of the rear rotor is much larger than the front rotor, which agrees with the mechanism of the aerodynamic interactions

between the front and rear rotors. However, the aerodynamic interference is beneficial to the front rotor in low to medium speeds, but with small magnitudes. The induced power of the rear rotor decreases with the forward speed, and the profile power increases. At high speed flight, the increase in the front rotor profile power becomes more pronounced, even without aerodynamic interference. The rotor induced and profile powers are much larger than the helicopter rotor, which indicates that the efficiency is lower than the helicopter rotor at high speed flight.

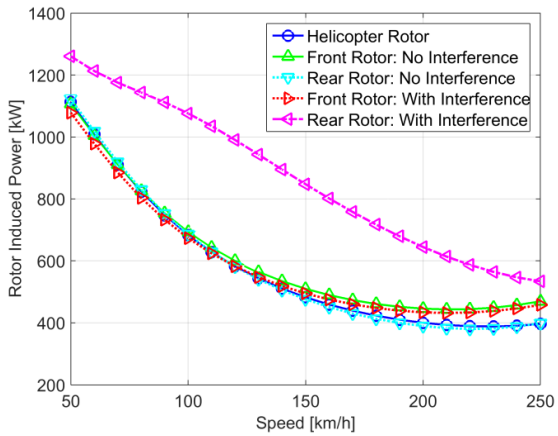

(a) induced power

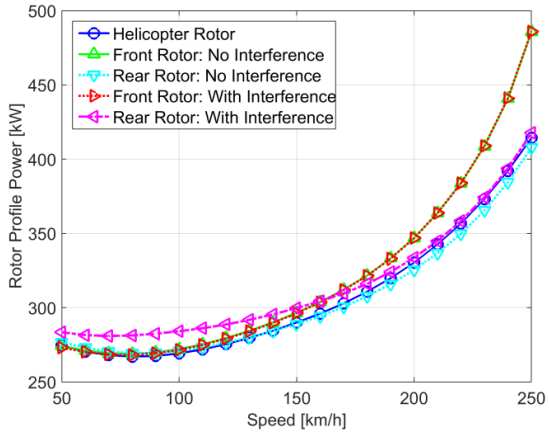

(b) profile power

Figure 8 Rotor induced and profile powers with forward speed.

The previous analysis indicates that the quadrotor aircraft operates in a more severe aerodynamic environment than the helicopter rotor, which increases the rotor profile and induced powers. Without the aerodynamic interference, this phenomenon is still pronounced at high speed flight. A major design feature of the quadrotor aircraft is the remove of the cyclic pitch controls from the rotor systems. The cyclic controls can adjust the distribution of the lift between the advancing and retreating sides, and control the tilt of the rotor disk plane. Figure 9 shows the steady blade flapping with the azimuth at a speed of 250km/h, and the aerodynamic interference between the front and rear rotors is included. The rotors of the quadrotor aircraft have much larger blade flapping than helicopter rotors. The phase difference between the helicopter and quadrotor aircraft is distinct. The phase corresponding to the maximum flapping of the quadrotor is close to the minimum flapping of the helicopter rotor. This phase difference is close to 180°. The rotor disk of the quadrotor aircraft is tilting backward, which can lead to a tilt of the rotor thrust and corresponding increase in the rotor drag. In the blade retreating side, the rotor blades of the quadrotor are flapping downward, which can cause an increase in the angle of attack. That is the reason why the angle of attack at the retreating side of the quadrotor aircraft is much large. The helicopter rotors use the cyclic pitch controls to overcome these shortcomings.

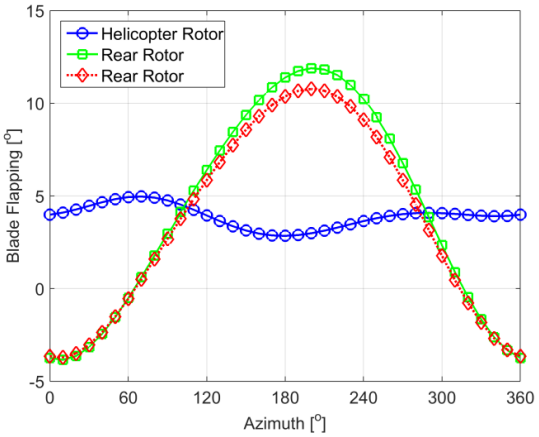

Figure 9 Steady blade flapping.

It is obvious that blade flapping decreases the aerodynamic efficiency of the rotors of the quadrotor aircraft. The helicopter rotor uses cyclic pitch to alleviate the severe aerodynamic environment. The cyclic pitch can be beneficial for quadrotor aircraft too. Figure 10 shows the rotor power of the quadrotor aircraft with longitudinal or lateral cyclic pitch angles at a speed of 250km/h. The power reduction is defined as the difference between the value at the pitch of 0° and the value with a longitudinal or lateral cyclic pitch control divided by the helicopter rotor power. It is obvious that the longitudinal or lateral cyclic pitch can effectively reduce the rotor power. The lateral cyclic pitch control θ_{1c} has the potential in reducing more power consumption. If the cyclic pitch controls of the helicopter rotor at a speed of 250km/h are used ($\theta_{1c} = 2.97°$ and $\theta_{1s} = -6.58°$), the front and rear rotor powers can be reduced by 13.1% and 8.32%. It can therefore be expected that more power can be saved by optimizing the cyclic pitch controls. Another benefit of applying cyclic pitch controls in the rotor systems of quadrotor aircraft is the increase in the maximum forward speed. From the

previous analysis, it can be concluded that uncontrolled blade flapping can lead to an increase in the rotor power at high speed flight.

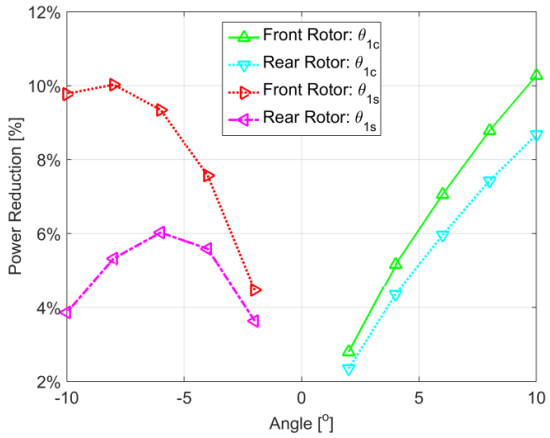

Figure 10 The effect of the cyclic pitch angles on the power reduction.

4. VARIABLE ROTOR SPEED

For comparison, the prescribed collective pitch of the quadrotor aircraft is set to 8°, 9°, 10°, 11°, and 12°, respectively. In the following analysis, aerodynamic interference is included. Figure 11 shows the collective pitches with the forward speed.

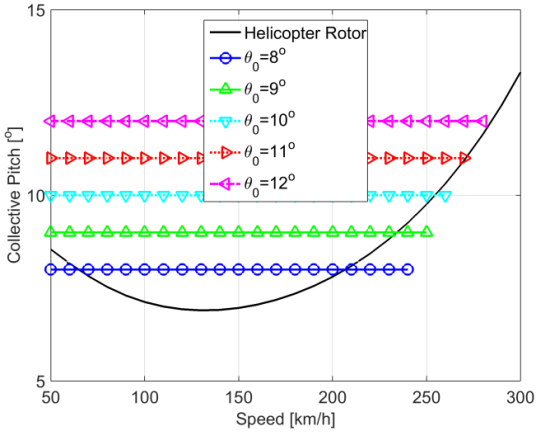

Figure 11 Variable collective pitch with forward speed.

Figure 12 shows the rotor speeds with the forward speed for different prescribed collective pitches. With increasing the forward speed, the rotor speeds of the front and rear rotors generally decrease first, and then increase. Increasing the prescribed collective pitch leads to a decrease in the rotor speed, and the rotor advance ratio increases. This can increase the aerodynamic asymmetry between the blade advancing and retreating sides of the rotors. Naturally, the maximum forward speed decreases with reducing the prescribed collective pitch. For smaller collective pitch, the rotor speed has to be larger to generate enough thrust. The increase in rotor speed leads to the increase in the blade tip speed, which limits the maximum forward speed.

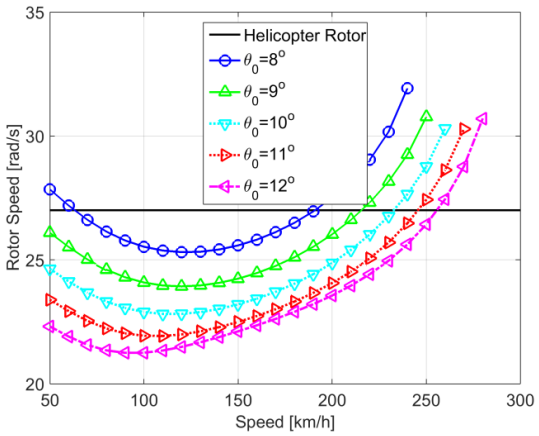

(a) front rotor

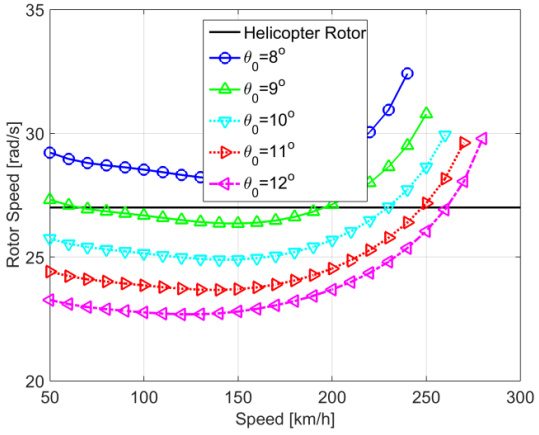

(b) rear rotor

Figure 12 Rotor speed with forward speed for different prescribed collective angles.

Figure 13 shows the longitudinal tilt of the fuselage with forward speed for different prescribed collective pitch angles. The longitudinal tilt of the quadrotor aircraft is much larger than the helicopter, which indicates that larger rotor drag is generated by the quadrotor aircraft. Larger longitudinal tilt means larger fuselage parasitic power. Increasing the prescribed collective pitch leads to the increase in the longitudinal tilt.

Figure 14 shows the rotor drag with the forward speed for different prescribed collective pitch. This is similar to Figure 6. The rotor drag of the quadrotor aircraft is much larger than the helicopter rotor, which leads to much larger longitudinal tilt. Increasing the prescribed collective pitch leads to an increase in the rotor drag, which means the deterioration of the aerodynamic environment around the rotors.

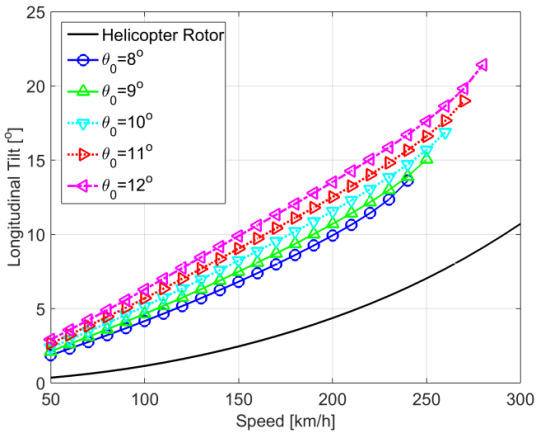

Figure 13 Longitudinal tilt with forward speed for different prescribed collective angles.

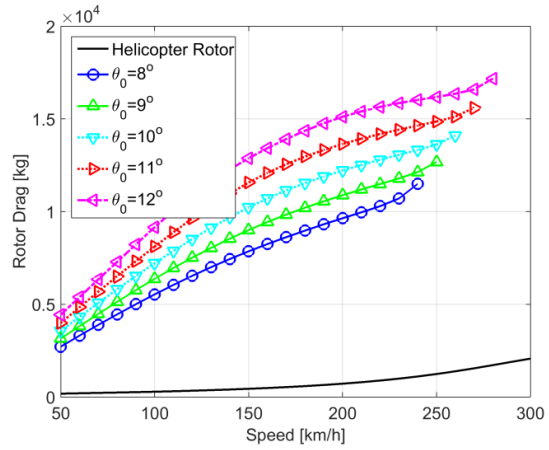

(a) front rotor

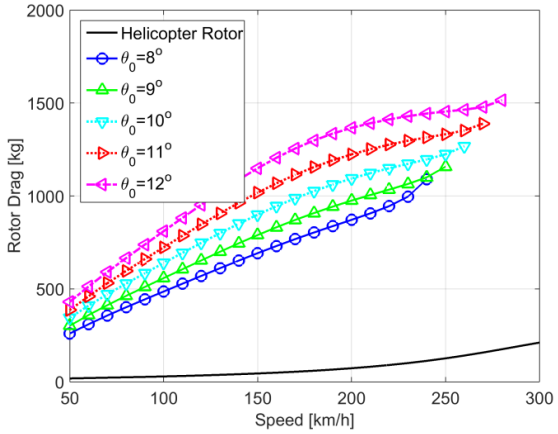

(b) rear rotor

Figure 14 Rotor drag with forward speed for different prescribed collective angles.

Figure 15 shows the longitudinal blade flapping with forward speed for different prescribed collective angles. The rotor disk of the helicopter tilts forward, but the rotor disks of the quadrotor aircraft tilt backward. The large backward tilt can lead to large rotor drags shown in Figure 14. Generally, the front rotor has larger longitudinal blade flapping than the rear rotor at a same prescribed collective pitch, which indicates that the front rotor generated larger rotor drag. Increasing the prescribed collective pitch results in an increase in the longitudinal flapping, since the lower rotor speed corresponding to the larger collective pitch results in more severe aerodynamic asymmetry between the advancing and retreating sides of the rotor disk.

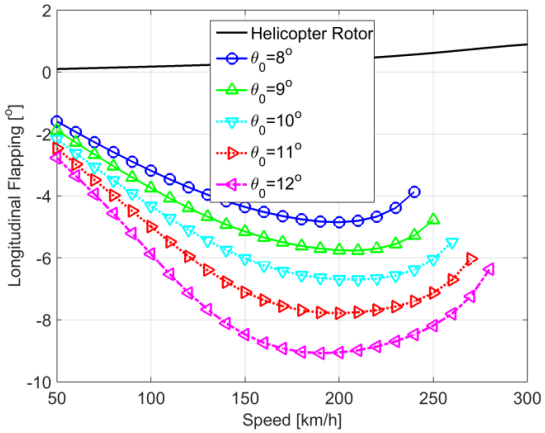

(a) front rotor

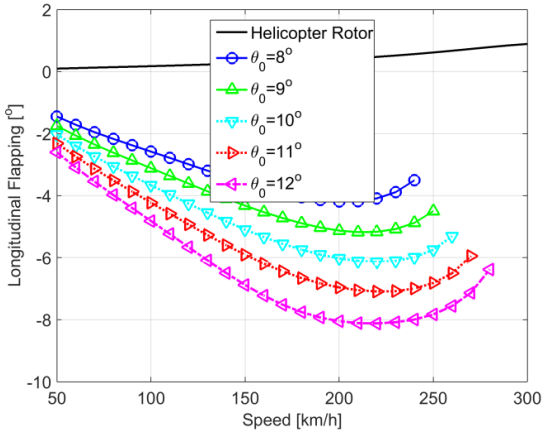

(b) rear rotor

Figure 15 Longitudinal flapping with forward speed for different prescribed collective angels.

Figure 16 shows the distribution of the angle attack at a speed of 250km/h and collective pitch of 10°. Different from Figure 7, the angle of attack in the retreating side is not large, and the stall is not develped. Figure 12 shows that the rotor speed of the quadrotor aircraft at this state is much larger than the helicopter rotor, so the angle of attack decreases. At a speed of 250km/h and collective pitch of 10°, the rotor speed is 28.8rad/s, and the corresponding Mach number at the blade tip in the advancing side is 0.90. As the rotor speed changes to 30.3rad/s at a speed of 260km/h, the corresponding Mach number is 0.94. It can be concluded that the compressibility effect at the blade tip limits the maximum speed of the quadrotor aircraft using the control method of varying rotor speed.

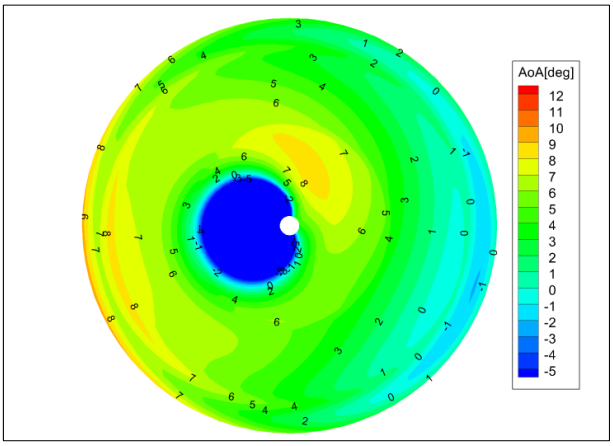

(a) front rotor

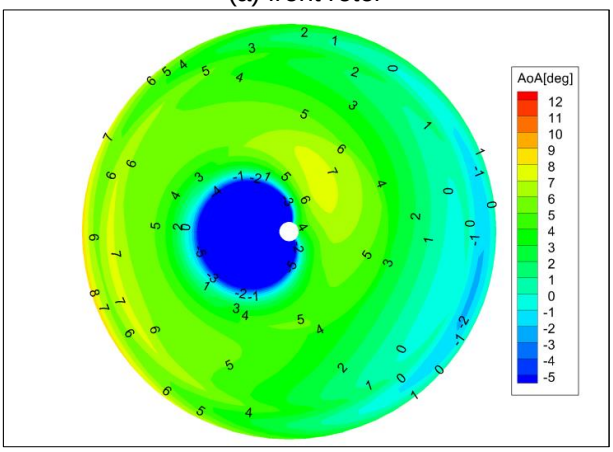

(b) rear rotor

Figure 16 Distribution of the angle attack at a speed of 250km/h and collective pitch of 10°.

Figure 17 shows the rotor thrust with forward speed for different prescribed collective angels. The front rotor thrust decreases first, and then increases. On the contrary, the rear rotor thrust increases, and then decreases. This trend is because of the variation of the resultant pitching moment acting on the quadrotor aircraft. At low speed flight, the nose up pitching moments generated by the rotors are larger than the nose down moment generated by the fuselage. The rear rotor needs to generate larger thrust than the front rotor to balance the nose up pitching moment. At medium to high speed flight, the direction of the resultant pitching moment changes, and the rear rotor has to generate a lower thrust. For the front rotor, the thrust decreases with increasing the prescribed collective pitch, and the rear rotor increases. However, the magnitudes are relatively small. Increasing the prescribed collective pitch has substantially small influence on the rotor thrusts.

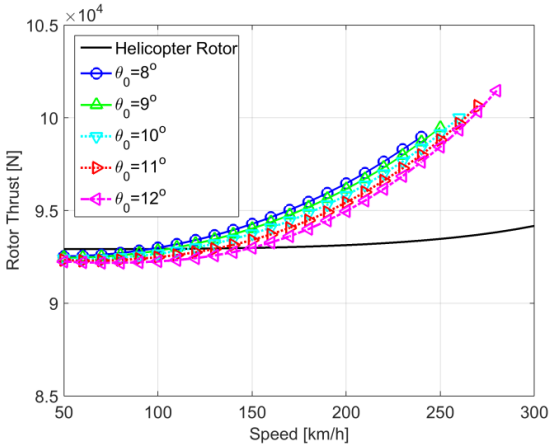

(a) front rotor

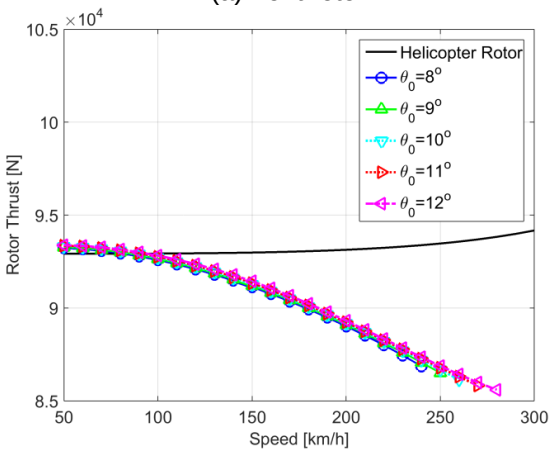

(b) rear rotor

Figure 17 Rotor thrust with forward speed for different prescribed collective angels.

Figure 18 shows the rotor power with forward speed for different prescribed collective angles. The figure indicates the following conclusions:

1) At low speed flight, increasing the collective pitch means the decrease in the rotor speed. Lower rotor speed can lead to the reduction of the rotor profile power [21, 22]. The rotor power consumption decreases.

2) At medium speed flight, the rear rotor has larger power consumption than the front due to the aerodynamic interference. The change of the front rotor power is substantially small, and the rear rotor power decreases with increasing the collective pitch. With a large collective pitch of 12°, the front rotor power can increase, but the rear rotor power still decreases by a very small decrement. Figure 19 shows the distribution of the angle attack at a speed of 150km/h and collective pitch of 12°. It is clear that the retreating side of the front rotor sees a much larger angle of attack, which indicates that it is about to undergo stall. The stall area is much larger than the rear rotor. Figure 12 shows that the front rotor has a much smaller rotor speed than the rear rotor at the speed of 150km/h. This leads to larger angle of attack and more severe aerodynamic

asymmetry. That is the reason why the rotor power increases with a larger collective pitch at a medium forward speed.

3) At high speed flight, the rotors of the quadrotor aircraft have a larger power consumption than the helicopter rotor. Since the aerodynamic interference has a smaller influence on the front rotor, the increase in the rotor power of the front rotor primarily comes from blade flapping. The increase in the rear rotor power comes from the aerodynamic interference and uncontrolled blade flapping. Increasing the prescribed collective pitch, which means the reduction of the rotor speed, can decrease the power at high speed flight. It can also increase the maximum forward speed.

4) Compared with Figure 3, the rotor power using variable rotor speed larger or smaller than the rotor using variable blade pitch depends on the prescribed rotor speed and collective pitch. Different prescribed collective angles can lead to an increase or decrease in the rotor power.

5) It can be concluded that using a large prescribed collective pitch is preferred from the point of view of flight performance. The major side effect is a possible power increase at a medium speed due to the lower rotor speed.

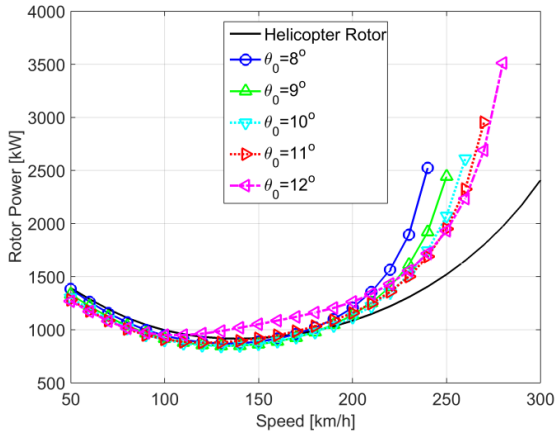

(a) front rotor

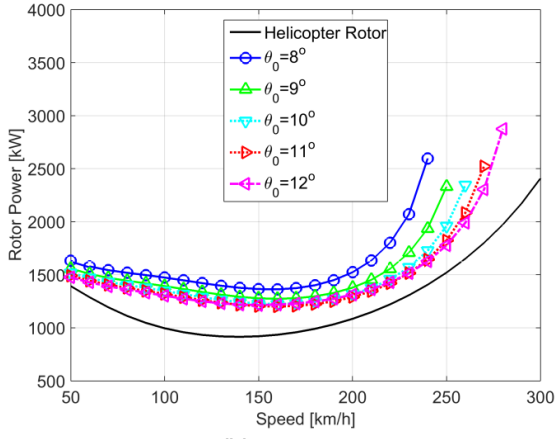

(b) rear rotor

Figure 18 Rotor power with forward speed for different prescribed collective angles.

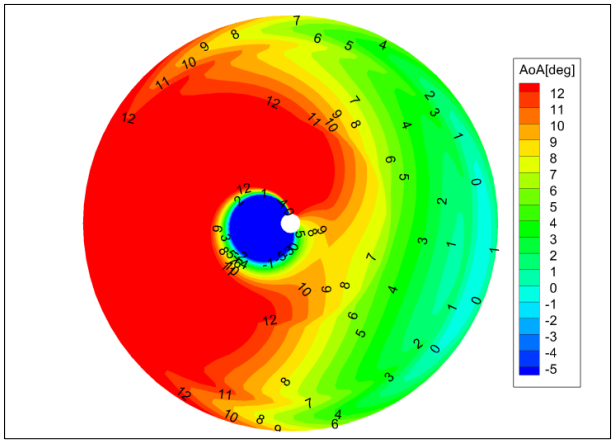

(a) front rotor

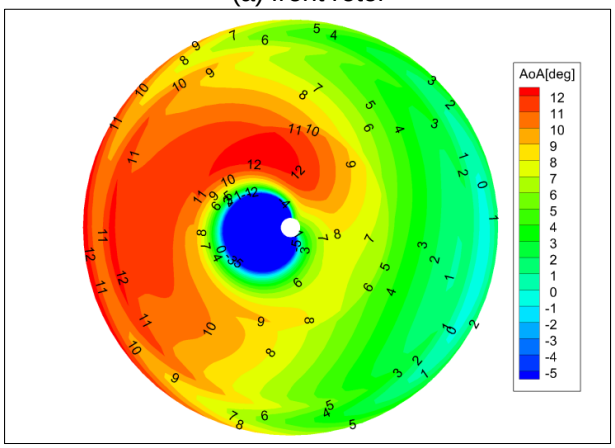

(b) rear rotor

Figure 19 Distribution of the angle attack at a speed of 150km/h and collective pitch of 12°.

Figure 20 shows the rotor profile power with the forward speed for different prescribed collective angles. The rotor profile power generally decreases with the forward speed, and then increases, except for the front rotor at medium speeds. At low speed flight, increasing the prescribed rotor collective can distinctly decrease the profile power. At medium speeds, this works for the rear rotor, but not for the front rotor. Since too low rotor speed can incur severe stall problem in the blade retreating side, as shown in Figure 19, the front rotor profile power can increase. At high speeds, increasing the collective leads to a decrease in the power consumption and an increase in the maximum forward speed.

Figure 21 shows the rotor induced power with the forward speed for different prescribed collective angels. The aerodynamic interference is beneficial to the front rotor at low speed flight, but the magnitude is small. It has strong influence on the rear rotor. At low speed flight, the increase in the power is caused by the aerodynamic interference, and the prescribed rotor collective pitch has little influence on the rotor induced power. At medium speeds, the collective pitch has substantially small

influence on the induced power. At high speeds, the effect becomes pronounced, and increasing the prescribed collective pitch can reduce the induced power.

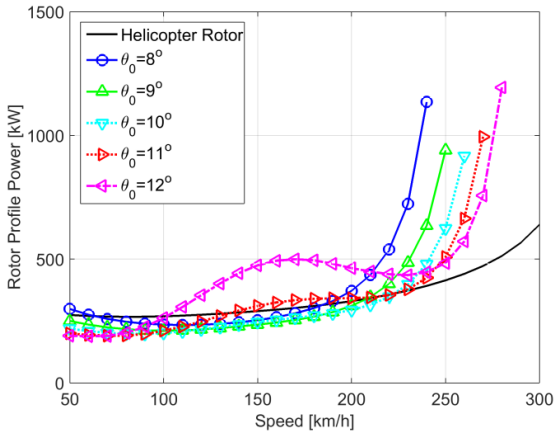

(a) front rotor

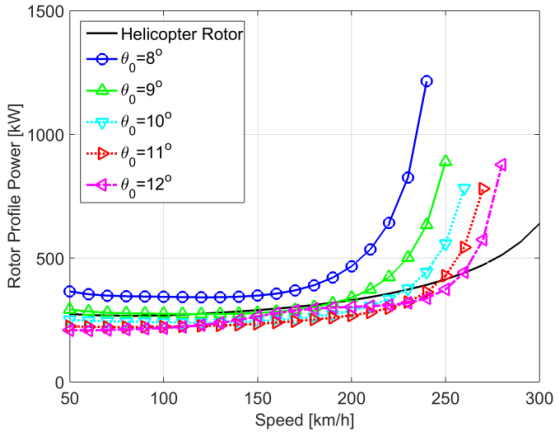

(b) rear rotor

Figure 20 Rotor profile power with forward speed for different prescribed collective angels.

The previous analysis indicates that using cyclic pitch controls is an effective way to reduce the rotor power at high speed flight. Figure 22 shows the power reduction by the cyclic pitch controls at a speed of 250km/h and collective pitch of 10º. It is clear that the cyclic control can effectively reduce the rotor power, especially the lateral cyclic pitch control. At a lateral cyclic pitch control of 10º, the front and rear rotor powers can be reduced by 17.1% and 15.4%, respectively. It can be expected that more power can be saved by optimizing the cyclic pitch controls. Another benefit of applying the cyclic pitch controls in the rotor systems of quadrotor aircraft is an increase in the maximum forward speed.

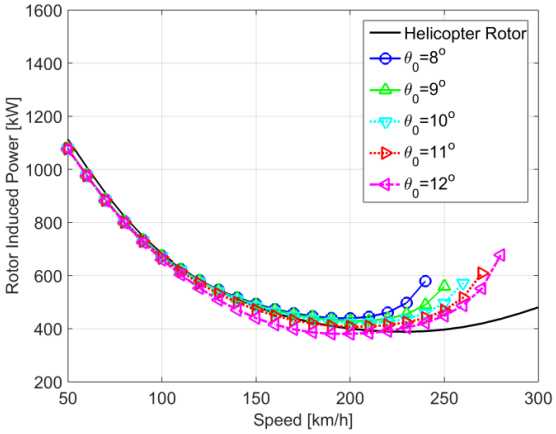

(a) front rotor

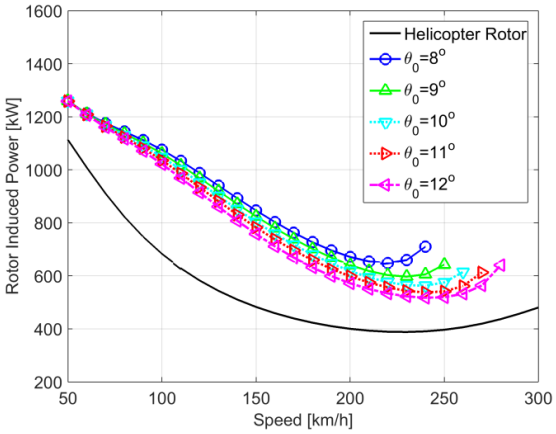

(b) rear rotor

Figure 21 Rotor induced power with forward speed for different prescribed collective angles.

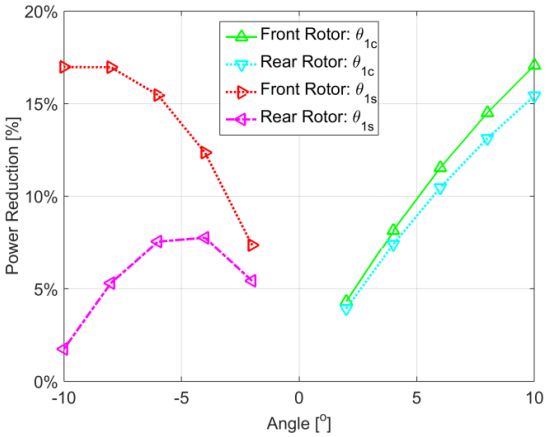

Figure 22 Power reduction by cyclic pitch control at a speed of 250km/h.

At a speed of 150km/h and a prescribed collective pitch of 12º, the front rotor power can be significant. Figure 23 shows the effect of the cyclic pitches on the rotor power at that flight state. It is clear that the cyclic pitches can reduce the rotor power, and the overall power reduction percentage is a little smaller than what is shown in Figure 22. Different from the mechanism at high speed flight, the longitudinal cyclic reduced the blade pitch in the

retreating side to decrease the angle of attack to alleviate the stall effect at a medium speed. At high speed flight, the angle of attack in the retreating side is small, as shown in Figure 16. The increase in the angle of attack can improve rotor performance. The strategy of applying cyclic pitch controls is different for different flight states.

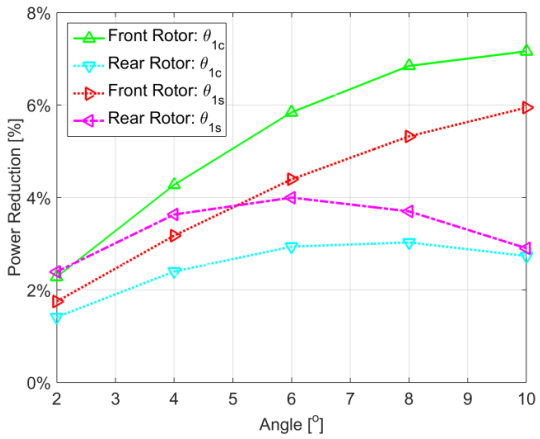

Figure 23 Power reduction by cyclic pitch control at a speed of 150km/h.

5. CONCLUSIONS

This work focused on the investigation of design features of quadrotor aircraft different from helicopters from the point of view of flight performance. A performance model considering the whole aircraft trim, blade flapping, and aerodynamic interference between the front and rear rotors is used to analyze the flight performance of a square formation quadrotor. By using the formation symmetry of quadrotor aircraft, the six equilibrium equations are reduced to three, and an iterative algorithm is proposed to obtain the converged solution of the equations. The analyses yielded the following conclusions:

1) The major design features of quadrotor aircraft different from helicopters are the uncontrolled blade flapping and the aerodynamic interference between the front and rear rotors from the point of view of flight performance. These lead to the overall rotor power consumption of quadrotor aircraft larger than the equivalent helicopter rotor.

2) Uncontrolled blade flapping can lead to the backward tilt of the rotor disk, which causes an increase in the rotor drag, especially at high speed flight. The increased rotor drag leads to an increase in the forward tilt of the fuselage, which can cause an increase in the parasitic power. The uncontrolled blade flapping also leads to an increase in the angle of attack in the blade retreating side, which can degrade the aerodynamic performance and the corresponding increase in the rotor profile and induced powers.

3) The aerodynamic interference is beneficial to the front rotor with a small magnitude, and can lead to the power increase in the rear rotor. In general, the aerodynamic interferences between the rotors lead to the increase in the total power of quadrotor aircraft.

4) The cyclic pitch controls can be used in the rotor systems of quadrotor aircraft to effectively reduce the power consumption. The strategy of applying cyclic pitch controls can be different for different flight state. The lateral cyclic pitch is more effective in reducing the rotor power than the longitudinal cyclic pitch control at high speed flight.

5) For varying rotor speed, using a larger prescribed collective pitch can be beneficial for power saving, except for the front rotor at medium speed flight. The larger prescribed collective pitch leads to much lower rotor speed, which can increase the rotor profile power due to the stall in the blade retreating side.

6) Compared with the helicopter rotor, from low to medium speed flight, the aerodynamic interference between the front and rear rotors dominates the power change. At high speed flight, both the uncontrolled blade flapping and aerodynamic interference can lead to the increase in the rotor power, and the uncontrolled blade flapping can become more pronounced.

ACKNOWLEDGMENTS

This work is supported from the National Natural Science Foundation of China (11972181), the Open Research Foundation of the Key Rotor Aerodynamics Laboratory (2005RAL20200104) and the Six Talent Peaks Project in Jiangsu Province (GDZB-013).

REFERENCES

[1] Cutler, M., How, J. P., “Analysis and Control of a Variable-Pitch Quadrotor for Agile Flight,” Journal of Dynamic Systems, Measurement and Control, Transactions of the ASME, Vol. 137, No. 10, 2015, pp. 101002.

[2] Sheng, S., and Sun, C., “Control and Optimization of a Variable-Pitch Quadrotor with Minimum Power Consumption,” Energies, Vol. 9, No. 4, 2016, pp. 1-18.

[3] Niemie, R., and Gandhi, F., “Multirotor Controls, Trim, and Autonomous Flight Dynamics of Plus- and Cross-Quadcopters,” Journal of Aircraft, Vol. 54, No. 5, 2017, pp. 1910-1920.

[4] Estelles, S., Tomas-Rodriguez, “Quadrotor Multibody Modelling by Vehiclesim: Adaptive Technique for Oscillations in a PVA Control System,” Journal of Vibration and Control Vol.

23, No. 16, 2017, pp. 2704–2723.
[5] Miranda-Colorado, R., Aguilar, L. T., Herrero-Brito, J. E. “Reduction of Power Consumption on Quadrotor Vehicles via Trajectory Design and a Controller-Gains Tuning Stage,” Aerospace Science and Technology, Vol. 78, 2018, pp. 280-296.
[6] Sun, S.,de Visser,C. C., and Chu, Q., “Quadrotor Gray-Box Model Identification from High-Speed Flight Data,”Journal of Aircraft, Vol. 56, No. 2, 2019, pp. 645-661.
[7] Luo, J., Zhu, L., and Yan, G., “Novel Quadrotor Forward-Flight Model Based on Wake Interference,” AIAA Journal, Vol. 53, No. 12, 2015, pp. 3522-3533.
[8] Hwang, J. Y., Jung, M. K., and Kwon, O. J., “Numerical Study of Aerodynamic Performance of a Multirotor Unmanned-Aerial-Vehicle Configuration,” Journal of Aircraft, Vol. 52. No. 3, 2015, pp. 839-846.
[9] Misiorowski, M., Gandhi, F., and Oberai, A. A., “Computational Study on Rotor Interactional Effects for a Quadcopter in Edgewise Flight,” AIAA Journal, Vol. 57, No. 12, 2019, pp. 5309-5319.
[10] Nguyen, D. H., Liu, Y., and Mori, K., “Experimental Study for Aerodynamic Performance of Quadrotor Helicopter,” Tans. Japan Soc. Aero. Space Sci., Vol. 61, No. 2, 2018, pp. 29-39.
[11] Niemiec, R. , and Gandhi, F., “Effects of Inflow Model on Simulated Aeromechanics of a Quadrotor Helicopter,” Proceedings of the American Helicopter Society 72nd Annual Forum, American Helicopter Soc. International, Alexandria, VA, May 17–19, 2016, pp. 3435-3447.
[12] McKay, M. E., Niemiec, R. , and Gandhi, F., “Performance Comparison of Quadcopters with variable-RPM and Variable-Pitch Rotors,” Journal of the American Helicopter Society, Vol. 64, No. 4, 2019, pp. 0420061-04200614.
[13] Peters, D. A. and HaQuang N., “Dynamic Inflow for Practical Application,” Journal of the American Helicopter Society, Vol. 33, No. 4, 1988, pp. 64-68.
[14] Han, D., Dong, C, and Barakos, G. N., “Performance Improvement of Variable Speed Rotors by Gurney Flaps,” Aerospace Science and Technology, Vol. 81, 2018, pp. 118-127.
[15] Han, D. and Barakos, G. N., “Aerodynamic Interference Model for Multi-Rotors in Forward Flight,” Journal of Aircraft, Vol. 57, No. 6, 2020, pp. 1220-1223.
[16] Leishman, J. G., Principles of Helicopter Aerodynamics, 2nd ed., Cambridge Univ. Press, Cambridge, New York, USA, 2006.
[17] McCormick, B. W., “Aerodynamics of V/STOL Flight,” Academic Press Inc., New York, USA, 1967, pp. 148-152.
[18] Yeo, H., Bousman, W.G. and Johnson, W., “Performance Analysis of a Utility Helicopter with Standard and Advanced Rotors,” Journal of the American Helicopter Society, Vol. 49, No. 3, 2004, pp. 250-270.
[19] Hilbert, K. B., “A Mathematical Model of the UH-60 Helicopter,” Technical Report NASA-TM-85890, 1984.
[20] Davis, S. J., “Pedesign Study for a Modern 4-Bladed Rotor for the RSRA,” Technical Report NASA-CR-166155, 1981.
[21] Kang, H., Saberi, H., and Gandhi, F., “Dynamic blade shape for improved helicopter rotor performance,” Journal of the American Helicopter Society, Vol. 55, No. 3, 2010, pp. 32008.
[22] Han, D., and Barakos, G. N., “Variable-speed Tail Rotors for Helicopters with Variable-speed Main Rotors,” Aeronautical Journal, Vol. 121, No. 1238, 2017, pp. 433-448.